

Classification of Aerosol over Central Europe by Cluster Analysis of Aerosol Columnar Optical Properties and Backward Trajectory Statistics

Artur SZKOP, Aleksander PIETRUCZUK, and Michał POSYNIAK

Institute of Geophysics, Polish Academy of Sciences, Warsaw, Poland;
e-mails: aszkop@igf.edu.pl, alek@igf.edu.pl (corresponding author),
mpos@igf.edu.pl

Abstract

A cluster analysis is applied to the Aerosol Robotic Network (AERONET) data obtained at Belsk, Poland, as well as three nearby Central European stations (Leipzig, Minsk and Moldova) for estimation of atmospheric aerosol types. Absorption Ångström exponent (AAE), aerosol optical thickness (AOT) and extinction Ångström exponent (EAE) parameters are used. Clustering in both 2D (AOT, EAE) and 3D (AOT, EAE, AAE) is investigated. A method of air mass backward trajectory analysis is then proposed, with the receptor site at Belsk, to determine possible source regions for each cluster. Four dominant aerosol source regions are identified. The biomass burning aerosol source is localized in the vicinity of Belarusian-Ukrainian border. Slovakia and northern Hungary are found to be the source of urban/industrial pollutants. Western Poland and eastern Germany are the main sources of polluted continental aerosols. The most differentiated source region of Scandinavia, Baltic Sea and Northern Atlantic, associated with lowest values of AOT, corresponds to clean continental and possibly maritime type aerosols.

Key words: aerosol optical properties, aerosol classification, cluster analysis, backward air mass trajectory, aerosol's origin determination.

1. INTRODUCTION

Aerosols have been observed in the global scale for more than a decade by both ground-based (Holben *et al.* 1999, 2001) and satellite (King *et al.* 1999, Kaufman *et al.* 2002, Mishchenko *et al.* 2007) remote sensing instruments. In the recent years, several classification schemes have been introduced to determine aerosol's type (Omar *et al.* 2009, Pappalardo *et al.* 2013). These new classification methods allow for better understanding of aerosols' origin and their source regions as well as aerosol modification during long range atmospheric transport. Moreover, knowledge of the aerosol type allows for a validation and a parametrization of aerosol models and satellite data (*e.g.*, Ginoux *et al.* 2001, Levy *et al.* 2007, Remer *et al.* 2005).

Aerosols are classified using satellite data by backtracking plumes to their probable source regions and analyzing satellite data products like fire locations or variation of optical properties (Russell *et al.* 2014). Another approach utilizes classification of aerosols based on their optical properties measured by both satellite and/or ground based measurements (Torres *et al.* 2002, Kaufman *et al.* 2002, Chin *et al.* 2002). One of the most commonly used databases containing aerosol optical properties is the Aerosol RObotic NETwork (AERONET) (Holben *et al.* 2001). This database, containing long series of optical properties for worldwide locations, allows to calculate radiative properties of various aerosols based on the location of the measurements site (*e.g.*, Dubovik *et al.* 2002, Cattrall *et al.* 2005). Relations between measured optical properties are also used to classify aerosols. The most commonly used method of finding aerosol type is the analysis of aerosol optical thickness (AOT) and its spectral dependence described by extinction Ångström exponent (EAE) (*e.g.*, Kalapureddy *et al.* 2009, Boselli *et al.* 2012). Analysis of extinction Ångström exponent and its derivative with respect to the wavelength is also used to classify aerosols (Gobbi *et al.* 2007) as well as combination of this method with LIDAR retrievals (Perrone *et al.* 2014). Moreover, LIDAR based parameters like LIDAR ratio, color ratio or depolarization are factors applied for the aerosol classification (Burton *et al.* 2012, Groß *et al.* 2013, 2015). In recent years, aerosol absorption parameters also have become one of the most promising factors for the aerosol classification. Costabile *et al.* (2013) used aerosol size distribution and spectral dependence of aerosol scattering and absorption to identify aerosol types. Giles *et al.* (2012) have shown that spectral dependence of aerosol absorption and extinction is useful for distinguishing between urban/industrial, biomass burning and mineral dust aerosols. The aforementioned method was used by Valenzuela *et al.* (2015) to identify dust over Granada. Clustering of aerosol properties combined with air mass' backward trajectory analysis was also used to classify aerosols, *e.g.*, Kikas *et al.* (2008).

In this paper, statistical analysis of AERONET retrievals for the period of 2001-2012, taken at four Central European stations (Belsk, Leipzig, Minsk, and Moldova), is used to determine the dominant aerosol types in the region. The utilized optical parameters include Aerosol Optical Thickness (AOT), Extinction Ångstrom Exponent (EAE) and Absorption Ångstrom Exponent (AAE). Moreover, a statistical analysis of air mass' backward trajectories is utilized for the Belsk station to determine probable source regions of the retrieved aerosol types. Source regions obtained by 3D (AOT *versus* EAE *versus* AAE) and 2D (EAE *versus* AOT) clustering are compared to these obtained from the fixed thresholds in the domain of EAE *versus* AOT. This allows for a direct comparison of all the classification methods as well as a preliminary identification of the best one for identification of aerosols originating from identified source regions.

2. INSTRUMENTATION AND METHODS

CIMEL Sun and Sky scanning photometers are used worldwide in determining aerosol optical properties by the Aerosol Robotic Network. The instruments provide aerosol optical thickness at several wavelengths derived from the direct Sun measurements as well as other optical parameters, *e.g.*, size distribution, refractive index and single scattering albedo (SSA), derived from sky radiance measurements. Detailed description of the instrument, data products and data processing are given by Holben *et al.* (1999, 2006), Eck *et al.* (1999), and Smirnov *et al.* (2000). In this work daily averaged, quality assured AERONET Level 2.0 aerosol optical thicknesses and single scattering albedo as well as parameters describing their spectral dependence are used. Uncertainties of AOT are estimated to vary from ± 0.01 in the visible and near infrared to ± 0.02 in the UV range (Holben *et al.* 1999, Eck *et al.* 1999). Uncertainties of single scattering albedo were estimated to be ± 0.03 for AOT greater than 0.4 at 440 nm (Dubovik *et al.* 2000). However, in the case of data level 2.0 this uncertainty could in fact be smaller, see discussion given by Giles *et al.* (2012).

Wavelength dependence of AOT is described by the extinction Ångstrom exponent (EAE) parameter:

$$\text{EAE} = - \frac{d \ln(\text{AOT}(\lambda))}{d \ln(\lambda)} \quad (1)$$

which is constant in the visible range. Small values of EAE typically indicate coarse aerosols, while large values indicate the fine ones. Columnar aerosol absorption properties are described by the absorption aerosol optical thickness (AAOT) which could be calculated from AERONET products by:

$$\text{AAOT}(\lambda) = (1 - \text{SSA}(\lambda))\text{AOT}(\lambda) \quad (2)$$

Spectral dependence of AAOT is described by the absorption Ångström exponent parameter defined, similarly to the extinction one, as:

$$\text{AAE} = -\frac{d \ln(\text{AAOT}(\lambda))}{d \ln(\lambda)} \quad (3)$$

In this work values of EAE and AAE are computed by linear regression of logarithm of proper optical thickness *versus* logarithm of wavelength λ . Spectral dependence of AAOT for fine homogenous black carbon (BC) spheroids (soot) is proportional to $1/\lambda$ which indicates AAE close to one for BC particles (Bergstrom *et al.* 2002) while for brown carbon (BrC) values of AAE could be much larger (Moosmüller *et al.* 2009). In the case of non-homogenous particles of varying sizes the AAOT spectral dependence is not significantly influenced by the size of the particles (Berry and Percival 1986) but it can be a function of the particles' state and physical properties (Fuller *et al.* 1999). For instance, for a BC core shelled by other material, values of AAE could be smaller than one according to the calculations performed by Lack and Cappa (2010). Values of AAE as low as ~ 0.3 were found by Russell *et al.* (2010). However, AERONET derived AAE values significantly below one could also be caused by uncertainties in estimation of SSA, as it was discussed by Giles *et al.* (2012). Authors of the aforementioned paper found, based on AERONET data, that AAE varies from 1.5 to 2.3 for dust aerosol and from 1.1 to 1.8 for both urban/industrial and biomass burning aerosols. In our study a threshold is set at AAE value of 0.75, below which the cases are considered to be caused mainly by errors in the estimation of SSA.

In this work a clustering method is applied to the daily averaged AERONET data level 2.0 for Belsk (51°49'N, 20°48'E), Leipzig (51°N, 12°E), Minsk (53°N, 27°E), and Moldova (47°N, 28°E) stations situated in the Central Europe to distinguish between different types of aerosols. A typically used approach is a clustering of AOT and EAE (Boselli *et al.* 2012) or AAE and EAE (Giles *et al.* 2012). We propose to perform a 3D clustering of AOT (at 440 nm), EAE (440-870 nm), and AAE (440-870 nm) data set and compare this analysis to 2D clustering of AOT (at 440 nm) and EAE (440-870 nm). According to the t-test the mean values of AOT measured at Leipzig, Minsk and Moldova stations do not differ significantly from the Belsk mean. All that stations represent Central Europe and data collected by them are considered as one block. The total number of measurements in the dataset is 3954 and this dataset is used in 2D clustering. The SSA retrievals, required for AAE calculation in 3D clustering, are not always available in

the level 2.0 data, for which the uncertainties must remain below a superimposed threshold (Holben *et al.* 2006). The uncertainties of SSA retrievals increase for lower AOT values. In the dataset studied here SSA retrievals were found only for 681 cases. Moreover, our calculations of AAE yielded values smaller than one in a number of cases. As indicated in the previous paragraph values slightly below unity may occur for composite aerosol with a BC core whilst values much lower than one are caused mainly by errors in estimation of SSA. A threshold for AAE at 0.75 was chosen with values below it deemed unphysical. In the end the total number of the remaining data records used in the 3D analysis is 613. It is worth noting that no SSA retrievals were found in the studied level 2.0 AERONET data in the cases of AOT below 0.24. On the other hand SSA values were available for all measurements with AOT above 0.4. In an intermediate region between the aforementioned AOT values, the SSA values are only available for a part of the dataset.

The clustering is performed based on the Lloyd's algorithm, also known as the *k*-means method (Lloyd 1982). A prechosen number of *k* clusters, defined by the randomly seeded centroids, are populated by *n* observation points. Each *n*-th observation point is assigned to exactly one cluster based on its lowest point to centroid distance. The iterative algorithm then repositions the centroids to the average values of the observation points in a given cluster until the centroids remain stationary or a limit of the iterations is reached. Procedure is performed ten times for randomly distributed seeds and a case with best separation of clusters is used in subsequent analysis. The number of clusters is determined by means of silhouette analysis which allows to check data separation for each number of clusters and choose the number for best data separation between clusters (Rousseeuw 1987, Kaufman and Rousseeuw 1990). The chosen clustering algorithm assumes the distribution of the data points to be close to normal. Since the AOT values are typically closer to a log-normal distribution the logarithm of the AOT values is used for the clustering. Separation of the aerosol spectra to coarse and fine modes is expected to be extracted from AOT *versus* EAE domain. Aerosols containing carbon and mineral dust are expected to form a cluster in the domain of AAE *versus* EAE. Clusters characterized by different values of AOT, if obtained, could indicate aerosols of different concentrations which may be caused by different origins and sources. In our previous work large AOT values were typically concurrent with an advection of air mass from the east and the south direction (Jarosławski and Pietruczuk 2010, Pietruczuk and Chaikovsky 2012). Pietruczuk (2013) also observed large increase in the AOT during advection episodes from the south direction. Both of these findings indicate the existence of possible aerosol source regions in the aforementioned directions.

A statistical analysis of air mass trajectories calculated with HYSPLIT model (Stein *et al.* 2015) is performed in an attempt to identify possible source regions of the aerosols assigned to each individual cluster of aerosol optical properties. The Belsk station is chosen as a receptor site and only the corresponding AERONET measurements are chosen from the clustered dataset for the further analysis. Trajectories are computed, for the location of Belsk only, with the use of HYSPLIT model supplied by GDAS meteorological archives. In the case of gaps in the GDAS archives the FNL data are used. We used meteorological ensemble trajectories to reduce uncertainties. Five-day trajectories, with endpoints separated by 6-hour long intervals (6:00, 12:00, and 18:00 UTC) and ending at 500 m above ground level over Belsk, are used similarly to our previous works (Pietruczuk and Jarosławski 2013, Pietruczuk 2013). This altitude is representative for boundary layer where most of aerosols are transported. A trajectory is chosen when its time of arrival is within a day of a clustered AERONET measurement. The trajectories are then cast onto a two-dimensional $0.5^\circ \times 0.5^\circ$ grid positioned over Europe. The value of each individual grid point becomes equal to the total number of hours spent over it by the trajectories belonging to the given cluster population. The length of each individual trajectory (measured along the trajectory) is used for the normalization to compensate for the decrease of trajectory density with the growing distance from the receptor. Such a decrease, in the case of a sheaf of straight lines on a two-dimensional surface, is inversely proportional to range.

This is an unorthodox approach and it should be emphasized that it presents a significant deviation from the usual methods for trajectory analysis, that may be found in the literature (*e.g.*, Seibert *et al.* 1994, Stohl *et al.* 1995, Robinson *et al.* 2011, Dvorská *et al.* 2009). In the typically used methods a function of the parameter values measured at a receptor site is added to the grid points laying on the receptor site back-trajectory. The sums are then normalized by the total number of trajectories passing over, thus creating the mean value for the grid point. In this way a spatial distribution of the aerosol source for a receptor site is revealed. Such approach applied to AOTs favors areas associated with the largest AOTs registered at receptor site, Belarus and Ukraine in case of Belsk (Kabashnikov *et al.* 2014) whilst sources of other types of aerosols are in fact not seen in that analysis. The method proposed in this work is aimed at recognizing both sources and characteristics of aerosols identified over the receptor site.

Satellite data are also used in discussion of possible sources of aerosols. We used AOTs measured by Moderate Resolution Imaging Spectroradiometer (MODIS) instrument, as well as MODVOLC thermal anomalies. Thermal anomalies are high-temperature MODIS pixels which were used primarily to monitor volcanic activity (Wright *et al.* 2004). However, it is a

good tool for open fires monitoring. Such fires may have a natural or anthropogenic origin like an agricultural activity or exploitation of oil fields (fire torches burning excess natural gas). The latter also explains the presence of fire pixels over the North Sea as a high number of oil rigs are operating in this area.

3. RESULTS OF AERONET DATA ANALYSIS

3.1 3D clustering

Cluster analysis of AERONET level 2.0 data for four central European stations containing SSA indicated the existence of three distinguishable clusters. Statistical parameters of aerosol optical properties for each cluster are listed in Table 1. In addition, parameters for the Belsk station (the receptor site in the trajectory analysis) are calculated separately. The differences in the values of the means calculated for Belsk as well as the remaining stations do not exceed 5% and are within 1 standard deviation in all the cases. This indicates that Belsk is a typical station for European Plain and thus is affected by similar types of aerosols as the other above-mentioned sites. It allows us to use the clusters determined for all the stations (depicted in Fig. 1) for the analysis limited only to Belsk station. An example of such an analysis is presented in the next step.

Clusters 3 and 1, containing 385 and 159 cases, respectively, are characterized by similar mean values of both Ångström exponents and different magnitudes of AOT. Mean values of EAE around 1.60-1.70 are indicative of fine particles and AAE around 1.13-1.18 suggests that they contain carbon.

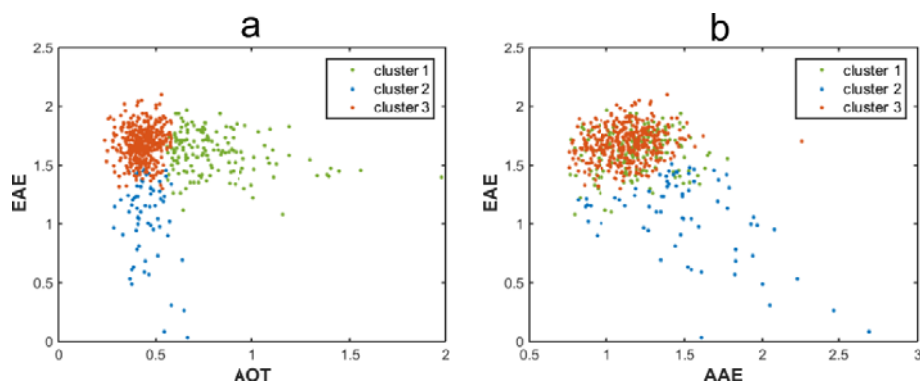


Fig. 1. The results obtained from the 3D clustering of AERONET data measured in the Central Europe (Belsk, Minsk, Moldova, and Leipzig). The results of the clustering, performed over 3-dimensional parameter space of AAE, EAE, and AOT, is projected on EAE *versus* AOT domain (a) and on EAE *versus* AAE domain (b).

Table 1

The results obtained from the 3D clustering. N is the cluster population size while Δ and δ are means and standard deviations, respectively

Dataset	Cluster	N	AOT at 440 nm		EAE		AAE	
			Δ	δ	Δ	δ	Δ	δ
All sites	1	159	0.80	0.26	1.60	0.18	1.18	0.21
	2	69	0.45	0.08	1.07	0.34	1.50	0.37
	3	385	0.43	0.07	1.69	0.14	1.13	0.18
Belsk	1	31	0.81	0.20	1.60	0.22	1.19	0.22
	2	9	0.46	0.09	1.23	0.19	1.49	0.30
	3	78	0.42	0.08	1.69	0.14	1.10	0.17

A little smaller AAE in cluster 3 indicates that the aerosol related to this cluster contains a larger carbon fraction. Simple classification scheme based on combination of AOT and EAE (*e.g.*, Barnaba and Gobbi 2004) suggests the presence of continental aerosols in both clusters characterized by different magnitudes of AOT which may indicate different types of continental aerosols. For example, Boselli *et al.* (2012), by performing 2D clustering, obtained a cluster of larger AOTs, around 0.21, and EAE around 1.61 which they identify as containing contaminated continental aerosol, *e.g.*, biomass burning or industrial. However, in our case, because of method's limitations, AOTs in clusters 3 and 1 are much higher (mean values of 0.43 and 0.8, respectively) than obtained by these authors, and significantly smaller than reported for biomass burning aerosols, where values larger than 1 are often seen (*e.g.*, Balis *et al.* 2003, Eck *et al.* 2003, Toledano *et al.* 2007, Hsu *et al.* 1999). In our case, cluster 1 could be related to biomass burning aerosol, while cluster 3 comprises continental aerosol of other types but also one containing carbon, like urban or industrial one. Cluster 2 of 69 cases is characterized by relatively small values of extinction Ångstrom exponent (mean EAE around 1), mean AOT around 0.45 and mean values of AAE around 1.5. This combination suggests the presence of mineral dust. The obtained values of AOTs and EAE are typical for Saharan dust events observed in the Mediterranean (Kaskaoutis *et al.* 2007a, Kosmopoulos *et al.* 2008, Kaskaoutis *et al.* 2007b) and AAE for mineral dust (Giles *et al.* 2012).

In order to find the possible aerosol source regions and identify aerosol types, a statistical analysis of backward trajectories was performed. The results of this analysis are shown in Fig. 2. In this work, trajectories ending over Belsk are used. Please note that an analysis was not performed for

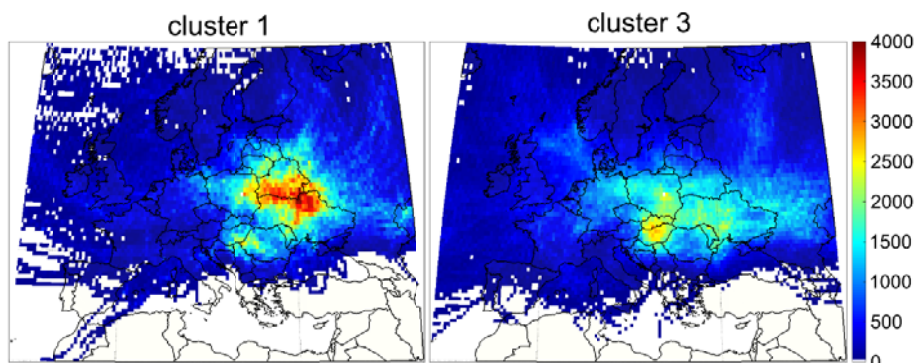


Fig. 2. The distribution of trajectories with endpoints (located at 500 m above the receptor) concurrent with the 3D clustered measurements for Belsk station. The values represent the number of hours spent by all the trajectories over a grid point, normalized by the lengths of individual trajectories (see Section 2). Clusters 1 and 3 are depicted. The population of cluster 2 is too small for this method of analysis, hence it is omitted here.

cluster 2, related to the mineral dust, because of an insufficient number of trajectories related to it (only 9 cases for the Belsk station dataset). Moreover, the chosen altitude of 500 m above the ground levels could be too small to investigate mineral dust over Belsk. For example, Saharan dust in the case of this station is rare and is registered typically in the free troposphere (Pietruczuk and Chaikovsky 2012). However, the number of records in clusters 1 and 3 is sufficient for a statistical analysis. Both of these clusters are related to fine, absorbing aerosols and the only difference is in the magnitude of AOT. Statistical analysis of the trajectories indicated different possible source regions of the aerosol, and thus probably different types of aerosols. In the case of cluster 1 with the largest AOT, typical for biomass burning events, the largest density of the trajectories corresponds to regions of seasonal biomass burning (Barnaba *et al.* 2011). Thus, cluster 1 is related to biomass burning aerosol. In the case of cluster 3, the largest density of trajectories is located over Slovakia and Hungary and also the existence of hot spots is indicated over Ukraine and in direct vicinity of Belsk. According to this analysis and our previous findings (Pietruczuk 2013), cluster 3 should be related to urban/industrial aerosol. The following results indicate to an underrepresentation of northern and western origin in the trajectory population. This stands in conflict with wind statistics for the Central Europe as the western winds are the most common for this region. In fact, more than 50% of backward trajectories is related to western direction. As the performed 3D clustering method excludes the cases with lower AOT values (where no SSA

value is available) these cases should include predominantly the underrepresented trajectory directions. Moreover, the limit of AOT renders the types of aerosols characterized by small values of AOT invisible in 3D clustering, *i.e.*, maritime, continental aerosol for clear conditions and even contaminated continental (Boselli *et al.* 2012). Such aerosols may still be analyzed through other methods, namely the 2D clustering and the fixed threshold approaches elaborated in the following paragraphs.

3.2 2D clustering

A 2D clustering is performed on all available daily averaged AERONET Level 2.0 data containing AOT and EAE measured at four stations used in the previous section. This analysis revealed 5 clusters; three of them correspond to that obtained by 3D clustering and two are related to smaller AOTs which are unavailable for 3D clustering. It is worth to note that the data used for 3D clustering are available only for AOT (at 440 nm) greater than 0.24. Moreover, not all of the data with AOTs between 0.24 and 0.4 fulfil conditions required for calculation of SSA Level 2.0 and because of that are not available for 3D clustering. The obtained clusters are depicted in Fig. 3 and the statistical parameters of aerosol optical properties related to the obtained clusters are listed in Table 2. The main differences, when comparing to the 3D clustering, are very sharp borders between the clusters which are well defined and may suggest good separation of the data. However, according to the performed silhouette analysis (Rousseeuw 1987, Kaufman and Rousseeuw 1990) separation of the clusters in this case is rather poor. Obtained borders seem to be artificial, which indicates a weak separation.

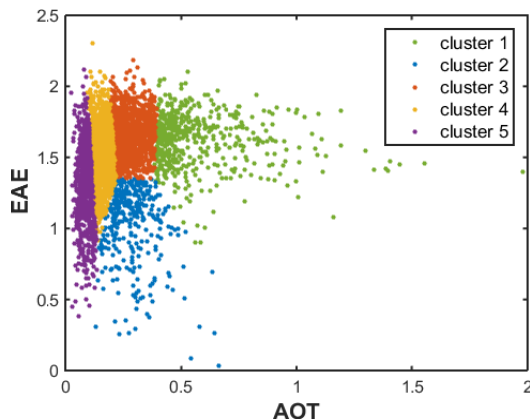


Fig. 3. The results obtained from the 2D clustering of AERONET data obtained at four locations in the Central Europe (Belsk, Minsk, Moldova, and Leipzig). The clustering was performed over a 2-dimensional parameter space of EAE and AOT.

Table 2

The results obtained from the 2D clustering. N is the cluster population size while Δ and δ are means and standard deviations, respectively

Dataset	Cluster	N	AOT		EAE	
			Δ	δ	Δ	δ
All sites	1	520	0.58	0.23	1.62	0.18
	2	336	0.29	0.08	1.04	0.26
	3	1100	0.28	0.05	1.66	0.15
	4	1248	0.16	0.03	1.53	0.20
	5	750	0.08	0.02	1.32	0.28
Belsk	1	100	0.58	0.19	1.61	0.20
	2	52	0.27	0.06	1.12	0.88
	3	246	0.28	0.05	1.66	0.15
	4	279	0.16	0.03	1.52	0.19
	5	146	0.09	0.02	1.29	0.26

Therefore, some points associated with a certain cluster may in fact belong to another one. This is probably caused by the use of only two parameters for clustering, which may not be enough to distinguish between types of aerosol characterized by similar optical properties. Another difference is a shift of cluster 1 into smaller AOTs direction and the presence of smaller AOTs in cluster 2.

The clusters related to smaller AOTs are numbered 4 and 5. AOTs related to cluster 5 are the smallest, with a mean value of 0.08 ± 0.02 , whilst EAE extends to the almost entire range with a mean value of 1.32 ± 0.28 , where assigned uncertainties are standard deviations for cluster. This cluster may contain two types of aerosol, depending on measured EAE. Aerosols characterized by small AOTs and large values of EAE are typically described as continental ones, whilst those characterized by small values of EAE are described by maritime ones. Mean AOT related to cluster 4 is equal or a little larger than 0.16 ± 0.03 , while the mean value of EAE is 1.53 ± 0.20 . Such a kind of aerosol may be described as polluted continental (Boselli *et al.* 2012) or mixed one (Russell *et al.* 2010). Cluster 3 is related to fine aerosol with comparatively larger AOTs of about 0.28 ± 0.05 which is much smaller than the one found in the 3D clustering. This, with the mean EAE values in the vicinity of 1.66 ± 0.15 , indicates that this cluster contains mainly cases of contaminated continental aerosol (Boselli *et al.* 2012) and industrial aerosol. This classification is also supported by the findings of Dubovik *et al.* (2002) where similar values (AOT of 0.26 and EAE between 1.2 and 2.3) were found for a station located in Paris and classified as “urban-industrial and

mixed” aerosol. According to other studies, *e.g.*, of Kalapureddy *et al.* (2009) or Pawar *et al.* (2015), this aerosol should be classified as urban/industrial. cluster 1, because of a possible misclassification of the data close to a sharp border, may contain also urban/industrial aerosol. However, as discussed in the previous section, larger values of AOT in this cluster should be related to biomass-burning aerosol. According to an analysis performed in the case of the 3D clustering, aerosol optical parameters related to cluster 2 indicate predominance of desert dust in this cluster.

As in the case of the 3D clustering, statistical analysis of backward trajectories was performed in order to find possible aerosol source regions and support identification of aerosol types. Trajectory densities related to each cluster are depicted in Fig. 4. In this case, many more trajectories related to cluster 2 were obtained. It allowed to perform an analysis for this cluster. The largest densities, obtained for the air mass coming from the southern and western directions, should not be equated to dust source. A transport of aerosol from this direction is rather accompanied by a transport of desert dust from northern Africa. Moreover, endpoints of trajectories at 500 m above ground level do not reflect typical altitude for dust observed over Belsk. In the case of cluster 1, the area with the largest trajectory density is similar to that obtained in case of the 3D clustering for both biomass-burning and urban/industrial aerosol. It should be expected because cluster 1 in the case of the 2D clustering is shifted towards smaller AOTs and contains some points that were associated with 3D cluster 3 described as continental aerosol containing carbon, industrial one. 2D cluster 3 is related to an advection of aerosol from the western direction rather than from the southern one. It is caused by shifting of this cluster to smaller AOTs as well as by presence of a large number of cases not present in the 3D clustering for which no SSA was available in the AERONET Level 2.0 data. Aerosols with smaller AOTs, related to this cluster and advection from the western direction (northern Germany and Benelux), should be classified mainly as mixed or polluted continental, while those with larger AOTs and advected from the southern direction should be classified as urban/industrial. High density of trajectories in the vicinity of the receptor site suggests that it is locally contaminated. However, in this case, the concept of “locality” may be extended onto western Poland and eastern Germany. In the case of cluster 4 no distinct source region is indicated. Latvia, Lithuania, and Estonia as well as advection from Atlantic are only slightly marked. According to analysis of aerosol optical properties, this cluster should be described rather as mixed one than polluted continental. Analysis of the trajectories related to cluster 5 indicates the northern part of the Baltic Sea and the North Sea as the most probable sources of aerosol. This cluster is not pure, and probably comprises more than one type of aerosol. Besides the potentially maritime aerosol (coarse

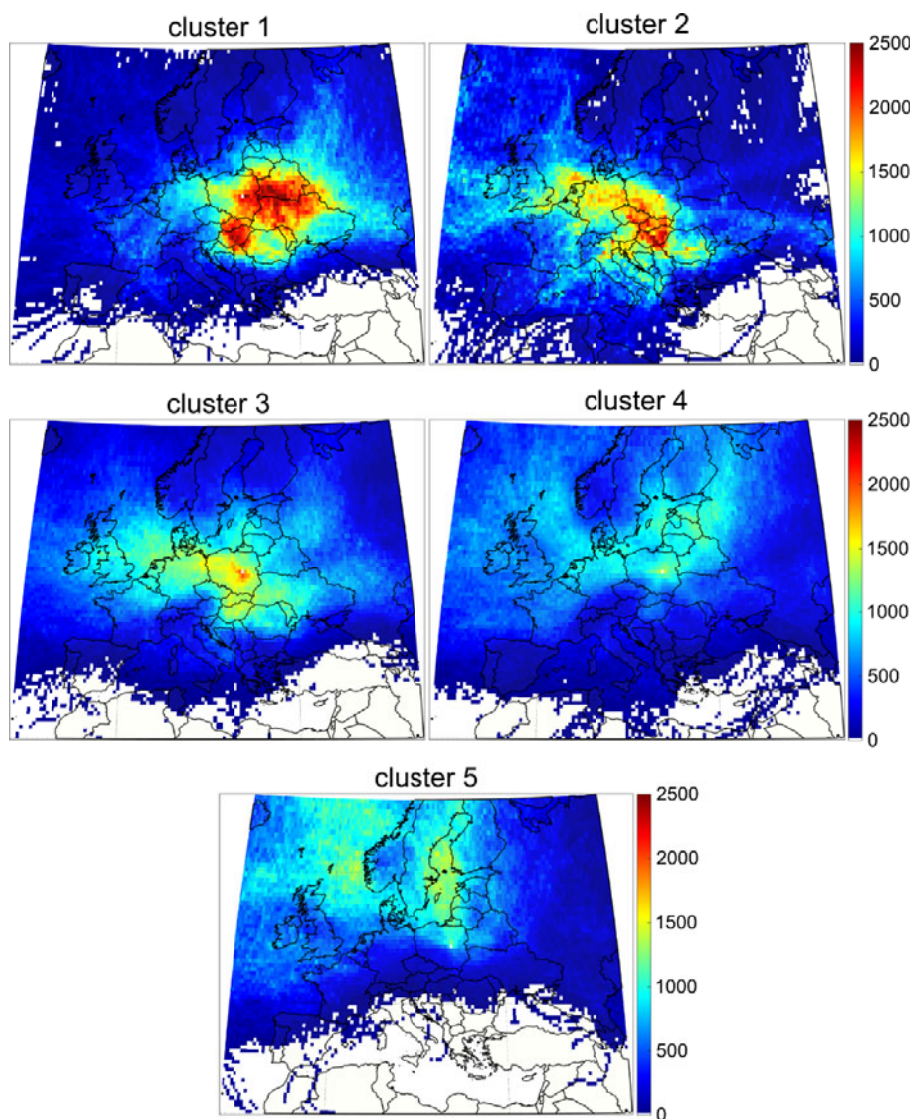


Fig. 4. The distribution of trajectories with endpoints (located 500 m above the receptor) concurrent with the 2D clustered measurements for Belsk station. The values represent the number of hours spent by all the trajectories over a grid point, normalized by the lengths of individual trajectories (see Section 2). Note different color scale than in Fig. 2.

particles with small AOTs), it contains continental aerosols (large values of EAE). This could be related to the advection of clear air mass, even cleaner than in the case of cluster 4 (see smaller AOTs). Maritime aerosol, if present,

should not be interpreted as salty water droplets but rather as an aerosol containing sea salt, as all the used trajectories are 5 day long and the mean lifetime of sea salt particles in the atmosphere is in the order of 5-6 days (Junge and Gustafson 1957, Koch *et al.* 2006). In the case of an absence of precipitation on the path from sea salt source to the receptor site, it is reasonable to assume that the coarse aerosol originating from mentioned regions is in fact a maritime aerosol containing sea salt. Additional trajectory analysis based on a fixed threshold of EAE is performed in the next section.

3.3 Threshold method

The differences between source regions obtained in the two previous subsections, as well as the desire to check source of coarse aerosol with small AOT, prompted us to perform additional analysis of trajectories supported by aerosol typing based on predefined levels of AOT and EAE. Such a typing may be found in the literature (Eck *et al.* 1999, Pace *et al.* 2006, Kaskaoutis *et al.* 2007a, b; Kaskaoutis *et al.* 2009, Kalapureddy *et al.* 2009, Pawar *et al.* 2015). We decided to use thresholds of AOT and EAE listed in Table 3 for the predefined types of aerosols; thresholds used by other authors are, for example, listed in work of Pawar *et al.* (2015). Synergy of the 2D and the 3D clustering with the analysis of backward trajectories allowed us to set thresholds in a way to distinguish between urban and biomass burning aerosols and obtain, as separate as possible, source regions in trajectory analysis. Such a differentiation between biomass burning and urban/industrial aerosol was not found in the aforementioned analyses based on fixed thresholds.

Table 3
The classification of the typical aerosol types occurring over Central Europe based on their optical properties

Cluster	AOT	EAE
Biomass burning	over 0.55	over 1.3
Urban/industrial	0.3 – 0.55	over 1.3
Saharan dust	over 0.3	up to 1
Continental	0 – 0.2	over 1.3
Maritime	0 – 0.2	up to 1

Results of the preformed trajectory analysis are shown in Fig. 5. Thanks to the carefully chosen threshold, distinguishing between biomass burning and urban/industrial aerosol, possible source regions of such aerosols are separated. The largest trajectory densities, related to mineral dust, should not be

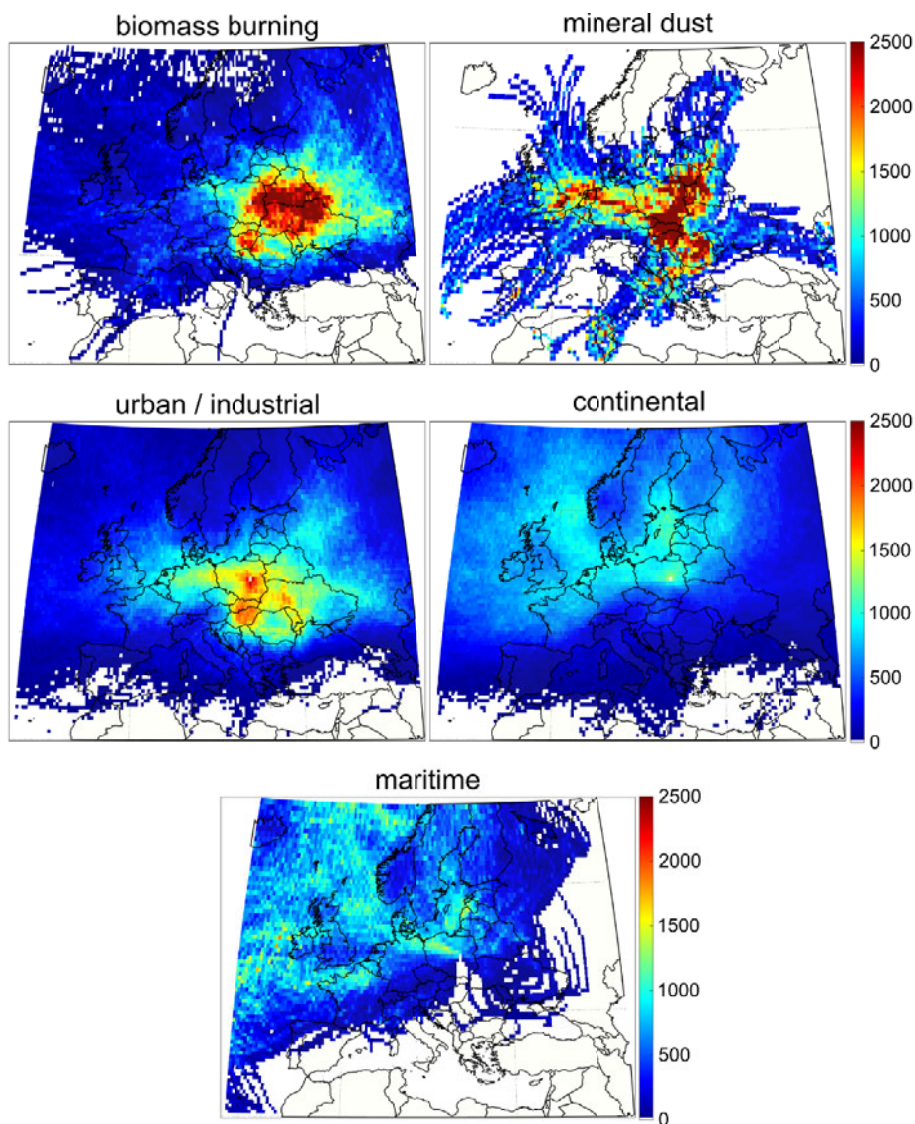


Fig. 5. Spatial density of the trajectories with endpoints (located 500 m above the receptor) concurrent with the fixed thresholds for AOT and EAE. Note different color scale than in Fig. 1.

interpreted as possible source regions as they correspond to a long-range transport, predominantly from northern Africa over typical paths of transport of mineral dust to Central Europe. Possible source regions obtained for continental aerosol are similar to those found for cluster 4 in the 2D clustering

with the addition of North Sea and English Channel regions. This may indicate that aerosol, which is in this case attributed to the continental type, is in fact partly related to a fast moving air mass deriving from North Sea/Northern Atlantic. Results of the trajectory analysis related to aerosol described as maritime one are the most noisy, however the concentration of trajectories is clearly seen over North Sea and Northern Atlantic, west of Ireland.

4. SOURCE REGIONS AND THE CORRESPONDING AEROSOL TYPES

The proposed methods for identification of potential source regions of various aerosol types were applied to data gathered over Belsk, Poland. The analysis yielded several potential source regions, including: (a) a region comprising the vicinity of Belarus-Ukraine border, (b) Slovakia and Hungary, (c) western Poland and eastern Germany, and (d) Scandinavia, Baltic Sea and widely understood Northern Atlantic, including Northern Sea. It must be stressed here that these identified source regions are not always strictly restricted to a single cluster/threshold originating from the aforementioned analysis methods but they rather represent a dominant source of aerosol with a given set of optical parameters.

Aerosol transported from the region (a) is characterized by the largest observed daily mean AOTs (>0.5), large mean values of EAE (~ 1.6), and AAE mean values of 1 which suggests significant load of fine, strongly absorbing aerosol. Advection of air mass from this direction is usually concurrent with significantly increased concentrations of PM₁₀ registered in central Poland (Pietruczuk and Jaroslowski 2013) and largest AOTs (Jaroslowski and Pietruczuk 2010, Kabashnikov *et al.* 2014). It should be mentioned that the correlation between AOT and PM₁₀ is found to be statistically insignificant for both Belsk and Warsaw (Zawadzka *et al.* 2013). Moreover, significant increase of AOTs are observed during transport of aerosol from the vicinity of Minsk to Belsk (Pietruczuk 2013), showing regions situated east of Poland to be significant sources of aerosol. Detailed analysis of MODVOLC fire pixels, thermal anomalies registered by MODIS instrument (Wright *et al.* 2004) presented in Fig. 6, indicate Ukraine as a region affected by wild fires of both natural and anthropogenic origin (seasonal burning of barren vegetation). MODVOLC pixel density in northern Ukraine and southern Belarus is not as high as in the case of south eastern Ukraine but this region is still strongly affected by the wildfires of similar mixed origin.

The source region (b) is surrounded by the Carpathian arch from the north and east. This orography, together with the dominance of western wind circulation, may favor accumulation of pollutions in this region. A number of possible sources of aerosol may be found at this region including the strongly urbanized and industrialized areas located next to Danube river, *i.e.*,

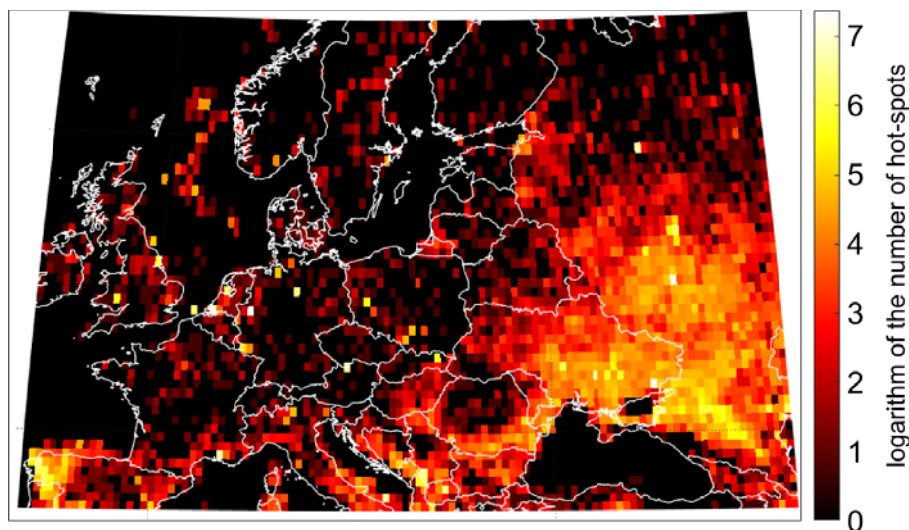


Fig. 6. Thermal anomalies over Europe obtained from MODVOLC algorithm; hot-spots at land are related to open fires and at the sea related to exploitation of oil fields. The data originates from MODIS (NASA) instrument for the 2000-2010 period.

Vienna, Bratislava, Budapest and heavy industry in the Kosice vicinity. Moreover, according to MODVOLC, biomass burning products may be transported from this region to central Poland. All that potential sources are clearly seen in Fig. 7 as hot spots of increased mean values of AOT taken by MODIS instrument and hot spots of MODVOLC thermal anomalies in Fig. 6. Advection of air mass from the south is typically related to increased PM10 concentrations and increased AOTs registered at Belsk. Although this region is a possible source of pollutants, the aerosol itself may be accumulated gradually as the air moves towards the receptor site. For example, a significant increase of AOT was observed during transport of aerosol from Vienna and Bratislava to Belsk over heavy industry dominated region situated near the Polish-Czech-Slovakian border (Pietruczuk 2013). It suggests that the industry south of central Poland, mainly in Upper Silesia and Ostrava regions, may be a significant aerosol source. This is supported by both of these regions being hot spots of exceeded permissible levels of particulate matter (EEA 2015).

The widely understood vicinity of the receptor site (c) should be also considered as a potential aerosol source. Hot spots of increased AOTs are clearly seen in western Poland and Saxony in eastern Germany; see Fig. 7. These are the densely populated areas surrounding Poznan, Lower Silesia region in Poland and Leipzig in Germany. Advection of relatively slow moving air mass from western direction is accompanied by observation of slight-

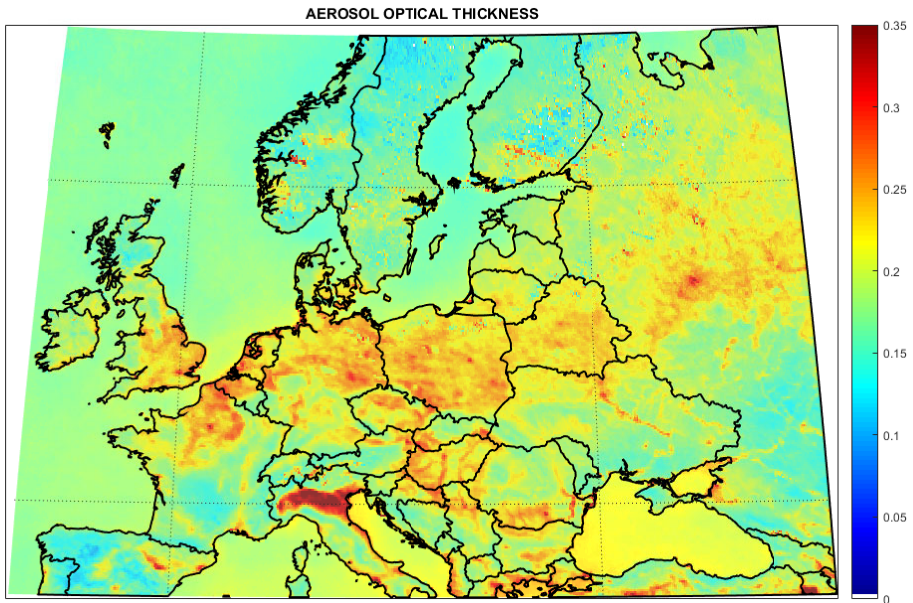


Fig. 7. Mean AOT at 500 nm over Europe obtained from the MODIS instrument (collection 6, L2), 2004-2015 period.

ly increased AOTs and PM₁₀ (Pietruczuk and Jaroslowski 2013). Such kind of aerosol represented by cluster 3 in the 2D analysis was named polluted continental. Its mean AOT is 0.28 and mean EAE is 1.66. It is worth to note that this aerosol was not found in the Section 3.3 because it is mixed-type aerosol with optical properties placed between urban/industrial and continental one. Advection of fast moving air mass from the west is accompanied by observation of small AOTs related to cluster 5 in 2D analysis or continental and maritime aerosols analyzed in Section 3.3.

The last source region (d) is the widest and most differentiated. The pattern for maritime aerosols partially overlaps that obtained for aerosol described as a continental one. For example, in the cluster 5 (2D analysis) a large portions of Baltic and North Sea are visible alongside the continental Europe. This indicates that both marine and continental type observations are related to advection of clear, fast moving air masses from western and northern directions. This makes distinguishing between maritime sources over Baltic Sea and Northern Atlantic and continental sources over Scandinavia and British Isles difficult. It should also be noted that the lifetime of maritime aerosol is relatively short. Model simulations presented by Jaegle *et al.* (2011) suggest that a lifetime of sea salt below 4 μm radius is in the 12-25 h range. In principle, this is a sufficient time, in the case of fast moving south-

bound trajectories, for aerosol to be transported above Belsk from the Baltic region. However, the mention of maritime aerosol in central or southern Poland may not be easily found in literature. Chemical analysis of $PM_{2.5}$ performed by Rogula-Kozłowska *et al.* (2012) in Zabrze (southern Poland) indicates that NaCl may constitute up to 5.8% of the ambient airborne dust during winter season and about 1.5% in the summer. The larger values of the NaCl fraction are expected in winter because chloride salts (both NaCl and KCl) are used in Poland to melt snow and ice on roads. However, the presence of NaCl in the summer $PM_{2.5}$ measurements may suggest that some sea salt is being transported as far as to the southern Poland. Moreover, the presence of the maritime aerosol should not be ruled out since the EAE values in cluster 5 are predominantly small, which is characteristic for this type of aerosol.

5. DISCUSSION AND CONCLUSIONS

The aforementioned analysis shows the existence of specific regions as potential sources of certain types of aerosols. However, aerosol typing based on statistical analysis of its optical properties alone may be insufficient to credibly distinguish the aerosol types for central Europe. Some of the obtained clusters may contain a mixture of different aerosol types. Such a cluster mixing occurs predominantly in the 2D clustering described in Section 3.2, where for example cluster 1 contains both biomass burning and urban/industrial aerosols. The cluster analysis applied on the AOT *versus* EAE space does not sufficiently separate aerosol types. This implies potential misclassification of aerosols with similar optical properties and consequently a poor separation of the potential source regions in the statistical analysis of the trajectories. The main drawback in this clustering approach is the lack of additional parameters for differentiating aerosols.

The significant non-zero skewness of AOT distribution may also be a limiting factor. Although the characteristic of this distribution is typically close to being log-normal, the low values dominate the data even when the logarithm of the AOT is considered. This causes the separation of aerosols characterized by small AOTs to be significantly better than in the case of aerosols with large AOT values. Therefore, we propose the use of an additional parameter (AAE) for differentiating aerosol types. Unfortunately, the retrieval of AAE is only available for large AOT cases and cloud-free conditions, whilst EAE is available for smaller AOTs and also in the case of broken clouds. Despite this limitation, a good separation of biomass burning, urban/industrial and mineral dust was obtained in Section 3.1, showing usefulness of this approach. A possible solution to the poor separation of aerosol types in both the 2D and the 3D clustering may be the use of fixed thresholds, as presented in Section 3.3. An introduction of disjoint, artificially im-

plemented, ranges of aerosol optical properties may overcome the problem associated with the misclassification of aerosols characterized by similar properties. A proper appointment of the ranges proves difficult, however, and requires additional knowledge of the aerosol types and properties within the studied dataset. In this analysis the results obtained from the 2D and, more importantly, the 3D clustering were used for a proper definition of the thresholds for the fixed range approach.

The aforementioned analysis was supported by a statistical analysis of backward air mass trajectories in order to determine the possible source regions and validate the identification of aerosol types. The obtained results are in a good agreement with our previous findings where the clustering was applied to the backward trajectories. However, clustering of the trajectories enabled us to find directions from which aerosols characterized by a certain set of optical properties were advected. In this work we define probable source regions of predominant aerosol types. Estimated source regions lay in the directions found in our previous works. The largest AOTs are related to an advection of air mass from the eastern and the southern directions (Jarosławski and Pietruczuk 2010, Pietruczuk 2013). Moreover, largest PM10 concentrations were registered at Belsk during advection episodes from the same directions (Pietruczuk and Jarosławski 2013). This agrees with the finding of this work that aerosols characterized by largest AOTs, biomass burning aerosols, have their possible source of origin between Belarus and Ukraine, which are located directly east of Belsk. Urban/industrial aerosols characterized by a little smaller AOTs, however still large, originate from Slovakia and Hungary located south of Belsk. According to our previous findings, the cleanest air episodes are typically related to an advection from Scandinavia and from over the Northern Atlantic. This work clarifies that most probable source of such kind of aerosols are Baltic and Northern Seas. Slow moving trajectories, arriving from the western direction, are related to accumulation of aerosol within the air mass traveling over heavily urbanized and industrialized regions in Western Europe (Pietruczuk and Jarosławski 2013, Pietruczuk 2013). This may be clearly seen in the analysis of backward trajectories related to cluster 4 as an increased density of the trajectories over Western Poland and Eastern Germany.

To summarize, three methods for identification of aerosol type based on its optical parameters were studied. It was found that, although applicable in some cases, these methods prove to be insufficient for a reliable identification scheme for all of the aerosol types occurring over Belsk, Poland. The use of an aerosol absorption parameter could possibly allow for a significantly better cluster separation and therefore for a more precise aerosol identification in most of the cases, provided the AAE parameter was available for all the AERONET measurements, including the low AOT ones. The pro-

posed auxiliary statistical analysis of backward air mass trajectories can provide the additional information regarding the aerosol in the form of its approximate source region or at least the general direction of the concurrent air advection. In the further studies of aerosols over Belsk, a synergy of statistical analysis of aerosol properties together with statistical analysis of backward trajectories should be used for aerosol classification.

Acknowledgments. This work was supported by the Polish National Science Centre under grant NCN 2013/09/B/ST10/03553. Authors would like to acknowledge AERONET station PIs: Albert Ansmann, Anatoli Chaikovsky, Piotr Sobolewski and Brent Holben for the use of the data from the AERONET stations. Authors also acknowledge the MODIS mission scientists and associated NASA personnel for the production of the data used in this research effort. The MODIS data were obtained from the Level-1 and Atmosphere Archive & Distribution System (LAADS).

References

- Balis, D.S., V. Amiridis, C. Zerefos, E. Gerasopoulos, M. Andreae, P. Zanis, A. Kazantzidis, S. Kazadzis, and A. Papayannis (2003), Raman lidar and sunphotometric measurements of aerosol optical properties over Thessaloniki, Greece during a biomass burning episode, *Atmos Environ.* **37**, 32, 4529-4538, DOI: 10.1016/S1352-2310(03)00581-8.
- Barnaba, F., and G.P. Gobbi (2004), Aerosol seasonal variability over the Mediterranean region and relative impact of maritime, continental and Saharan dust particles over the basin from MODIS data in the year 2001, *Atmos. Chem. Phys.* **4**, 9/10, 2367-2391, DOI: 10.5194/acp-4-2367-2004.
- Barnaba, F., F. Angelini, G. Curci, and G.P. Gobbi (2011), An important fingerprint of wildfires on the European aerosol load, *Atmos. Chem. Phys.* **11**, 20, 10487-10501, DOI: 10.5194/acp-11-10487-2011.
- Bergstrom, R.W., P.B. Russell, and P. Hignett (2002), Wavelength dependence of the absorption of black carbon particles: Predictions and results from the TARFOX experiment and implications for the aerosol single scattering albedo, *J. Atmos. Sci.* **59**, 3, 567-577, DOI: 10.1175/1520-0469(2002)059<0567:WDOTAO>2.0.CO;2.
- Berry, M.V., and I.C. Percival (1986), Optics of fractal clusters such as smoke, *J. Modern Optics* **33**, 5, 577-591, DOI: 10.1080/713821987.
- Boselli, A., R. Caggiano, C. Cornacchia, F. Madonna, L. Mona, M. Macchiato, G. Pappalardo, and S. Trippetta (2012), Multi year sun-photometer measurements for aerosol characterization in a Central Mediterranean site, *Atmos. Res.* **104**, 98-110, DOI: 10.1016/j.atmosres.2011.08.002.

- Burton, S.P., R.A. Ferrare, C.A. Hostetler, J.W. Hair, R.R. Rogers, M.D. Obland, C.F. Butler, A.L. Cook, D.B. Harper, and K.D. Froyd (2012), Aerosol classification using airborne High Spectral Resolution Lidar measurements—methodology and examples, *Atmos. Meas. Tech.* **5**, 1, 73-98, DOI: 10.5194/amt-5-73-2012.
- Catrrall, C., J. Reagan, K. Thome, and O. Dubovik (2005), Variability of aerosol and spectral lidar and backscatter and extinction ratios of key aerosol types derived from selected Aerosol Robotic Network locations, *J. Geophys. Res.* **110**, D10, DOI: 10.1029/2004JD005124.
- Chin, M., P. Ginoux, S. Kinne, O. Torres, B.N. Holben, B.N. Duncan, R.V. Martin, J.A. Logan, A. Higurashi, and T. Nakajima (2002), Tropospheric aerosol optical thickness from the GOCART model and comparisons with satellite and Sun photometer measurements, *J. Atmos. Sci.* **59**, 3, 461-483, DOI: 10.1175/1520-0469(2002)059<0461:TAOTFT>2.0.CO;2.
- Costabile, F., F. Barnaba, F. Angelini, and G.P. Gobbi (2013), Identification of key aerosol populations through their size and composition resolved spectral scattering and absorption, *Atmos. Chem. Phys.* **13**, 5, 2455-2470, DOI: 10.5194/acp-13-2455-2013.
- Dubovik, O., A. Smirnov, B.N. Holben, M.D. King, Y.J. Kaufman, T.F. Eck, and I. Slutsker (2000), Accuracy assessments of aerosol optical properties retrieved from Aerosol Robotic Network (AERONET) Sun and sky radiance measurements, *J. Geophys. Res.* **105**, D8, 9791-9806, DOI: 10.1029/2000JD900040.
- Dubovik, O., B. Holben, T.F. Eck, A. Smirnov, Y.J. Kaufman, M.D. King, D. Idier, T. Anre, and I. Slutsker (2002), Variability of absorption and optical properties of key aerosol types observed in worldwide locations. *J. Atmos. Sci.* **59**, 3, 590-608, DOI: 10.1175/1520-0469(2002)059<0590:VOAAOP>2.0.CO;2.
- Dvorská, A., G. Lammel, and I. Holoubek (2009), Recent trends of persistent organic pollutants in air in central Europe—Air monitoring in combination with air mass trajectory statistics as a tool to study the effectivity of regional chemical policy. *Atmos. Environ.* **43**, 6, 1280-1287, DOI: 10.1029/2000JD900040.
- Eck, T.F., B.N. Holben, J.S. Reid, O. Dubovik, A. Smirnov, N.T., O'Neill, I. Slutsker and S. Kinne (1999), Wavelength dependence of the optical depth of biomass burning, urban, and desert dust aerosols, *J. Geophys. Res.* **104**, D24, 31333-31349, DOI: 10.1029/1999JD900923.
- Eck, T.F., B.N. Holben, J.S. Reid, N.T. O'Neill, J.S. Schafer, O. Dubovik, A. Smirnov, M.A. Yamasoe, and P. Artaxo (2003), High aerosol optical depth biomass burning events: A comparison of optical properties for different source regions, *Geophys. Res. Lett.* **30**, 20, DOI: 10.1029/2003GL01786.
- EEA (2015), Air quality in Europe — 2015 report, European Environment Agency, DOI: 10.2800/62459.

- Fuller, K.A., W.C. Malm, and S.M. Kreidenweis (1999), Effects of mixing on extinction by carbonaceous particles, *J. Geophys. Res.* **104**, D13, 15941-15954, DOI: 10.1029/1998JD100069.
- Giles, D.M., B.N. Holben, T.F. Eck, A. Sinyuk, A. Smirnov, I. Slutsker, R.R. Dickerson, A.M. Thompson, and J.S. Schafer (2012), An analysis of AERONET aerosol absorption properties and classifications representative of aerosol source regions, *J. Geophys. Res.* **117**, D17, DOI: 10.1029/2012JD018127.
- Ginoux, P., M. Chin, I. Tegen, J.M. Prospero, B. Holben, O. Dubovik, and S.J. Lin (2001), Sources and distributions of dust aerosols simulated with the GOCART model, *J. Geophys. Res.* **106**, D17, 20255-20273, DOI: 10.1029/2000JD000053.
- Gobbi, G.P., Y.J. Kaufman, I. Koren, and T.F. Eck (2007), Classification of aerosol properties derived from AERONET direct sun data, *Atmos. Chem. Phys.* **7**, 2, 453-458, DOI: 10.5194/acp-7-453-2007.
- Groß, S., M. Esselborn, B. Weinzierl, M. Wirth, A. Fix, and A. Petzold (2013), Aerosol classification by airborne high spectral resolution lidar observations, *Atmos. Chem. Phys.* **13**, 5, 2487-2505, DOI: 10.5194/acp-13-2487-2013.
- Groß, S., V. Freudenthaler, M. Wirth, and B. Weinzierl (2015), Towards an aerosol classification scheme for future EarthCARE lidar observations and implications for research needs, *Atmos. Sci. Lett.* **16**, 1, 77-82, DOI: 10.1002/asl2.524.
- Holben, B.N., D. Tanré, A. Smirnov, T.F. Eck, I. Slutsker, O. Dubovik, F. Lavenu, N. Abuhassen, and B. Chatenet (1999), Optical properties of aerosols from long term ground-based aeronet measurements. **In:** *Proc. ALPS99, 17-23 January 1999, Meribel, France*, WK1-O-19.
- Holben, B.N., D. Tanre, A. Smirnov, T.F. Eck, I. Slutsker, N. Abuhassan, and G. Zibordi (2001), An emerging ground-based aerosol climatology: Aerosol optical depth from AERONET, *J. Geophys. Res.* **106**, D11, 12067-12097, DOI: 10.1029/2001JD900014.
- Holben, B.N., T.F. Eck, I. Slutsker, A. Smirnov, A. Sinyuk, J. Schafer, D. Giles, and O. Dubovik (2006), AERONET's version 2.0 quality assurance criteria. **In:** *Asia-Pacific Remote Sensing Symp.*, International Society for Optics and Photonics, 64080Q-64080Q, DOI: 10.1117/12.706524.
- Hsu, N.C., J.R. Herman, O. Torres, B.N. Holben, D. Tanre, T.F. Eck, A. Smirnov, B. Chatenet, and F. Lavenu (1999), Comparisons of the TOMS aerosol index with Sun-photometer aerosol optical thickness: Results and applications, *J. Geophys. Res.* **104**, D6, 6269-6279, DOI:10.1029/1998JD200086.
- Jaeglé, L., P.K. Quinn, T.S. Bates, B. Alexander, and J.T. Lin (2011), Global distribution of sea salt aerosols: new constraints from in situ and remote sensing observations, *Atmos. Chem. Phys.* **11**, 7, 3137-3157, DOI: 10.5194/acp-11-3137-2011.

- Jarosławski, J., and A. Pietruczuk (2010), On the origin of seasonal variation of aerosol optical thickness in UV range over Belsk, Poland, *Acta Geophys.* **58**, 6, 1134-1146, DOI: 10.2478/s11600-010-0019-4.
- Junge, C.E., and P.E. Gustafson (1957), On the distribution of sea salt over the United States and its removal by precipitation, *Tellus* **9**, 2, 164-173, DOI: 10.1111/j.2153-3490.1957.tb01869.x.
- Kabashnikov, V., G. Milinevsky, A. Chaikovsky, N. Miatselskaya, V. Danylevsky, A. Aculinin, D. Kalinskaya, E. Korchemkina, A. Bovchaliuk, A. Pietruczuk, P. Sobolevsky, and V. Bovchaliuk (2014), Localization of aerosol sources in East-European region by back-trajectory statistics, *Int. J. Remote Sens.* **35**, 19, 6993-7006, DOI: 10.1080/01431161.2014.960621.
- Kalapureddy, M.C.R., D.G. Kaskaoutis, P. Ernest Raj, P.C.S. Devara, H.D. Kambezidis, P.G. Kosmopoulos, and P.T. Nastos (2009), Identification of aerosol type over the Arabian Sea in the premonsoon season during the Integrated Campaign for Aerosols, Gases and Radiation Budget (ICARB), *J. Geophys. Res.* **114**, D17, DOI: 10.1029/2009JD011826.
- Kaskaoutis, D.G., P. Kosmopoulos, H.D. Kambezidis, and P.T. Nastos (2007a), Aerosol climatology and discrimination of different types over Athens, Greece, based on MODIS data, *Atmos. Environ.* **41**, 34, 7315-7329, DOI: 10.1016/j.atmosenv.2007.05.017.
- Kaskaoutis, D.G., H.D. Kambezidis, N. Hatzianastassiou, P.G. Kosmopoulos, and K.V.S. Badarinath (2007b), Aerosol climatology: on the discrimination of aerosol types over four AERONET sites, *Atmos. Chem. Phys.* **7**, 3, 6357-6411, DOI: 10.5194/acpd-7-6357-2007.
- Kaskaoutis, D.G., K.V.S. Badarinath, S. Kumar Kharol, A. Rani Sharma, and H.D. Kambezidis (2009), Variations in the aerosol optical properties and types over the tropical urban site of Hyderabad, India, *J. Geophys. Res.* **114**, D22, DOI: 10.1029/2009JD012423.
- Kaufman, L., and P.J. Rousseeuw (1990), *Finding Groups in Data: An Introduction to Cluster Analysis*, John Wiley and Sons Inc., Hoboken, DOI: 10.1002/9780470316801.
- Kaufman, Y.J., D. Tanré, and O. Boucher (2002), A satellite view of aerosols in the climate system, *Nature* **419**, 6903, 215-223, DOI: 10.1038/nature01091.
- Kikas, U., A. Reinart, A. Pugatshova, E. Tamm, and V. Ulevicius (2008), Microphysical, chemical and optical aerosol properties in the Baltic Sea region, *Atmos. Res.* **90**, 2, 211-222, DOI: 10.1016/j.atmosres.2008.02.009.
- King, M.D., Y.J. Kaufman, D. Tanré, and T. Nakajima (1999), Remote sensing of tropospheric aerosols from space: Past, present, and future, *Bull. Am. Meteorol. Soc.* **80**, 11, 2229-2259, DOI: 10.1175/1520-0477(1999)080<2229:RSOTAF>2.0.CO;2.
- Koch, D., G.A. Schmidt, and C.V. Field (2006), Sulfur, sea salt, and radionuclide aerosols in GISS ModelE, *J. Geophys. Res.* **111**, D6, DOI: 10.1029/2004JD005550.

- Kosmopoulos, P.G., D.G. Kaskaoutis, P.T. Nastos, and H.D. Kambezidis (2008), Seasonal variation of columnar aerosol optical properties over Athens, Greece, based on MODIS data, *Remote Sens. Environ.* **112**, 5, 2354-2366, DOI: 10.1007/s11270-013-1605-2.
- Lack, D.A., and C.D. Cappa (2010), Impact of brown and clear carbon on light absorption enhancement, single scatter albedo and absorption wavelength dependence of black carbon, *Atmos. Chem. Phys.* **10**, 9, 4207-4220, DOI: 10.5194/acp-10-4207-2010.
- Levy, R.C., L.A. Remer, and O. Dubovik (2007), Global aerosol optical properties and application to Moderate Resolution Imaging Spectroradiometer aerosol retrieval over land, *J. Geophys. Res.* **112**, D13, DOI: 10.1029/2006JD007815.
- Lloyd, S. (1982), Least squares quantization in PCM, *IEEE Trans Inform. Theor.* **28**, 2, 129-137, DOI: 10.1029/2006JD0078.
- Mishchenko, M.I., I.V. Geogdzhayev, B. Cairns, B.E. Carlson, J. Chowdhary, A.A. Lacis, and L.D. Travis (2007), Past, present, and future of global aerosol climatologies derived from satellite observations: A perspective, *J. Quant. Spectrosc. Rad. Trans.* **106**, 1, 325-347, DOI: 10.1016/j.jqsrt.2007.01.007.
- Moosmüller, H., R.K. Chakrabarty, and W.P. Arnott (2009), Aerosol light absorption and its measurement: A review, *J. Quant. Spectrosc. Rad. Trans.* **110**, 11, 844-878, DOI: 10.1016/j.jqsrt.2009.02.035.
- Omar, A.H., D.M. Winker, M.A. Vaughan, Y. Hu, C.R. Trepte, R.A. Ferrare, K.-P. Lee, C.A. Hostetler, Ch. Kittaka, R.R. Rogers, R.E. Kuehn, and Z. Liu (2009), The CALIPSO automated aerosol classification and lidar ratio selection algorithm, *J. Atmos. Ocean Technol.* **26**, 10, 1994-2014, DOI: 10.1175/2009JTECHA1231.1.
- Pace, G., A.D. Sarra, D. Meloni, S. Piacentino, and P. Chamard (2006), Aerosol optical properties at Lampedusa (Central Mediterranean). 1. Influence of transport and identification of different aerosol types, *Atmos. Chem. Phys.* **6**, 3, 697-713, DOI: 10.5194/acp-6-697-2006.
- Pappalardo, G., L. Mona, G. D'Amico, U. Wandinger, M. Adam, A. Amodeo, and A. Boselli (2013), Four-dimensional distribution of the 2010 Eyjafjallajökull volcanic cloud over Europe observed by EARLINET, *Atmos. Chem. Phys.* **13**, 8, 4429-4450, DOI: 10.5194/acp-13-4429-2013.
- Pawar, G.V., P.C.S. Devara, and G.R. Aher (2015), Identification of aerosol types over an urban site based on air-mass trajectory classification, *Atmos. Res.* **164**, 142-155, DOI: 10.1016/j.atmosres.2015.04.022.
- Perrone, M.R., F. De Tomasi, and G.P. Gobbi (2014), Vertically resolved aerosol properties by multi-wavelength lidar measurements, *Atmos. Chem. Phys.* **14**, 3, 1185-1204, DOI: 10.5194/acp-14-1185-2014.

- Pietruczuk, A. (2013), Short term variability of aerosol optical thickness at Belsk for the period 2002-2010, *Atmos. Environ.* **79**, 744-750, DOI: 10.1016/j.atmosenv.2013.07.054.
- Pietruczuk, A., and A. Chaikovsky (2012), Variability of aerosol properties during the 2007-2010 spring seasons over central Europe, *Acta Geophys.* **60**, 5, 1338-1358, DOI: 10.2478/s11600-012-0017-9.
- Pietruczuk, A., and J. Jarosławski (2013), Analysis of particulate matter concentrations in Mazovia region, central Poland, based on 2007-2010 data, *Acta Geophys.* **61**, 2, 445-462, DOI: 10.2478/s11600-012-0069-x.
- Remer, L.A., Y.J. Kaufman, D. Tanré, S. Mattoo, D.A. Chu, J.V. Martins, and B.N. Holben (2005), The MODIS aerosol algorithm, products, and validation, *J. Atmos. Sci.* **62**, 4, 947-973, DOI: 10.1175/JAS3385.1.
- Robinson, N.H., H.M. Newton, J.D. Allan, M. Irwin, J.F. Hamilton, M. Flynn, and H. Coe (2011), Source attribution of Bornean air masses by back trajectory analysis during the OP3 project, *Atmos. Chem. Phys.* **11**, 18, 9605-9630, DOI: 10.5194/acp-11-9605-2011.
- Rogula-Kozłowska, W., K. Klejnowski, P. Rogula-Kopiec, B. Mathews, and S. Szopa (2012), A study on the seasonal mass closure of ambient fine and coarse dusts in Zabrze, Poland, *Bull. Environ. Contam. Toxic.* **88**, 5, 722-729, DOI: 10.1007/s00128-012-0533-y.
- Rousseeuw, P.J. (1987), Silhouettes: a graphical aid to the interpretation and validation of cluster analysis, *Comput. Appl. Math.* **20**, 53-65, DOI: 10.1016/0377-0427(87)90125-7.
- Russell, P.B., R.W. Bergstrom, Y. Shinozuka, A.D. Clarke, P.F. De Carlo, J.L. Jimenez, J.M. Livingston, J. Redemann, O. Dubovik, and A. Strawa (2010), Absorption Angstrom exponent in AERONET and related data as an indicator of aerosol composition, *Atmos. Chem. Phys.* **10**, 3, 1155-1169, DOI: 10.5194/acp-10-1155-2010.
- Russell, P.B., M. Kacenelenbogen, J.M. Livingston, O.P. Hasekamp, S.P. Burton, G.L. Schuster, M.S. Johnson, K.D. Knobelspiesse, J. Redemann, S. Ramachandran, and B. Holben (2014), A multiparameter aerosol classification method and its application to retrievals from spaceborne polarimetry, *J. Geophys. Res.* **119**, 16, 9838-9863, DOI: 10.1002/2013JD021411.
- Seibert, P., H. Kromp-Kolb, U. Baltensperger, D.T. Jost, M. Schwikowski, A. Kasper, and H. Puxbaum (1994), Trajectory analysis of aerosol measurements at high alpine sites. **In:** *Proc. 4th EUROTRAC Symp. "Transport and Transformation of Pollutants in the Troposphere"*, 25-29 March 1996, Garmisch-Partenkirchen, Germany, 689-693.
- Smirnov, A., B.N. Holben, T.F. Eck, O. Dubovik, and I. Slutsker (2000), Cloud-screening and quality control algorithms for the AERONET database, *Remote Sens. Environ.* **73**, 3, 337-349, DOI: 10.1016/S0034-4257(00)00109-7.
- Stein, A.F., R.R. Draxler, G.D. Rolph, B.J.B. Stunder, M.D. Cohen, and F. Ngan (2015), NOAA's HYSPLIT atmospheric transport and dispersion modeling

- system, *Bull. Am. Meteorol. Soc.* **96**, 12, 2059-2077, DOI: 10.1175/BAMS-D-14-00110.1.
- Stohl, A., G. Wotawa, P. Seibert, and H. Kromp-Kolb (1995), Interpolation errors in wind fields as a function of spatial and temporal resolution and their impact on different types of kinematic trajectories, *J. Appl. Meteorol.* **34**, 10, 2149-2165, DOI: 10.1175/1520-0450(1995)034<2149:IEIWFA>2.0.CO;2.
- Toledano, C., V.E. Cachorro, A.M. De Frutos, M. Sorribas, N. Prats, and B.A. De la Morena (2007), Inventory of African desert dust events over the southwestern Iberian Peninsula in 2000-2005 with an AERONET Cimel Sun photometer, *J. Geophys. Res.* **112**, D21, DOI: 10.1029/2006JD008307.
- Torres, O., P.K. Bhartia, J.R. Herman, A. Sinyuk, P. Ginoux, and B. Holben (2002), A long-term record of aerosol optical depth from TOMS observations and comparison to AERONET measurements, *J. Atmos. Sci.* **59**, 3, 398-413, DOI: 10.1175/1520-0469(2002)059<0398:ALTROA>2.0.CO;2.
- Wright, R., L.P. Flynn, H. Garbeil, A.J.L. Harris, and E. Pilger (2004), MODVOLC: near-real-time thermal monitoring of global volcanism, *J. Volcanol. Geothermal Res.* **135**, 29-49, DOI: 10.1016/j.jvolgeores.2003.12.008.
- Valenzuela, A., F.J. Olmo, H. Lyamani, M. Antón, G. Titos, A. Cazorla, and L. Alados-Arboledas (2015), Aerosol scattering and absorption Angström exponents as indicators of dust and dust-free days over Granada (Spain), *Atmos. Res.* **154**, 1-13, DOI: 10.1016/j.atmosres.2014.10.015.
- Zawadzka, O., K.M. Markowicz, A. Pietruczuk, T. Zielinski, and J. Jaroslowski (2013), Impact of urban pollution emitted in Warsaw on aerosol properties. *Atmos. Environ.* **69**, 15-28, DOI: 10.1016/j.atmosenv.2012.11.065.

Received 8 March 2016

Received in revised form 26 September 2016

Accepted 18 October 2015